

Directional hearing in the barn owl (*Tyto alba*)

Roger B. Coles* and Anna Guppy*

Research School of Biological Sciences, Australian National University, Canberra, A.C.T. 2601, Australia

Accepted December 13, 1987

Summary. The acoustical properties of the external ear of the barn owl (*Tyto alba*) were studied by measuring sound pressure in the ear canal and outer ear cavity. Under normal conditions, pressure amplification by the external ear reaches about 20 dB between 3–9 kHz but decreases sharply above 10 kHz. The acoustic gain curve of the outer ear cavity alone is close to that of a finite-length exponential horn between 1.2–13 kHz with maximum gain reaching 20 dB between 5–9 kHz. Pressure gain by the facial ruff produces a maximum of 12 dB between 5–8 kHz and decreases rapidly above 9 kHz.

The directional sensitivity of the external ear was obtained from pressure measurements in the ear canal. Directivity of the major lobe is explained, to a first approximation, by the sound diffraction properties of a circular aperture. Aperture size is based on the average radius (30 mm) of the open face of the ruff. Above 5 kHz, the external ear becomes highly directional and there is a 26° disparity in elevation between the acoustic axis of the left and right ear. In azimuth, directivity patterns are relocated closer to the midline as frequency increases and the acoustic axis moves at a rate of 20°/octave between 2–13 kHz. Movement of the axis can be explained, to a first approximation, by the acoustical diffraction properties of an obliquely truncated horn, due to the asymmetrical shape of the outer ear cavity.

The directional sensitivity of the barn owl ear was studied by recording cochlear microphonic (CM) potentials from the round window membrane. Between 3–9 kHz, CM directivity patterns

are clearly different to the directivity patterns of the external ear; CM directionality is abruptly lost above 10 kHz. Above 5 kHz, CM directivity patterns are characterized by an elongated major lobe containing the CM axis, forming a tilted band of high amplitude but low directionality (*CM axial plane*), closely bordered by minima or nulls. The highest directionality is found in the *CM directional plane*, approximately perpendicular to the CM axial plane. The left and right ear axial planes are symmetrical about the interaural midline (tilted 12° to the right of the midline of the head) and inclined by an average of 60° to the left and right respectively. In azimuth, the CM axis moves towards the midline at a rate of 37°/octave as frequency increases from 2–9 kHz, crossing into contralateral space near 7 kHz. In the CM directional plane, the directivity of the major lobe suggests that a pressure gradient may occur at the TM. The region of frontal space mapped by movement of the CM axis in azimuth closely matches the angle of sound incidence which would be expected to produce the maximum driving pressure at the TM. It is suggested that acoustical interference at the TM results from sound transmission through the interaural canal and therefore the ear is inherently directional. It is proposed that ear directionality in the barn owl may be explained by the combined effect of sound diffraction by the outer ear cavity and a pressure gradient at the TM.

Abbreviations: CM cochlear microphonic; RMS root mean square; SPL sound pressure level; TM tympanic membrane

* Present address: Zoologisches Institut, Universität München, Luisenstrasse 14, 8 München 2, Federal Republic of Germany

Introduction

Owls are the most specialized birds for hearing and many species are remarkable for the bilateral asymmetry of the external ear which has been linked to a highly developed sense of directional

hearing (Stresemann 1934; Schwartzkopff 1962; Norberg 1968, 1977, 1978; Payne 1971). Sound localization has been studied extensively in the barn owl particularly at the behavioural and neural levels (for reviews see Knudsen 1980; Konishi 1983). The current theories of sound localization assume that the barn owl ear is a pressure receiver (Payne 1971; Knudsen and Konishi 1979; Knudsen 1980; Konishi 1983) and the directional mechanisms are thought to involve interaural intensity and time cues analyzed entirely by the central auditory pathway. It has been concluded that the perception of sound elevation depends on interaural intensity cues provided by the facial ruff and sound azimuth depends on interaural time cues arising from the physical separation of the two eardrums (Knudsen 1980; Konishi 1983).

A major problem in understanding directional mechanisms in birds generally is that hearing is restricted to frequencies usually well below 10 kHz. These wavelengths are poorly diffracted by the head and if the avian ear is regarded as a pressure receiver, yield small interaural intensity differences. The relatively small size of the head also reduces interaural time disparities to values well below 100 μ s. Nevertheless, the barn owl can locate live prey or a sound source in total darkness with a precision of 1°–5° in azimuth and elevation, relying on a narrow band of frequencies between 5–9 kHz (Payne 1971; Konishi 1973a, b; Knudsen et al. 1979). It has been calculated that the barn owl makes accurate judgements of sound location where the interaural time disparities are as small as 4 μ s (Knudsen 1980).

Apart from the current views on sound localization in the barn owl, an alternative mechanism is possible because directionally sensitive hearing can result from a pressure gradient at the tympanic membrane (TM). Such a mechanism was first proposed for insect ears (Autrum 1942) and experimental evidence is available for several arthropod species (for reviews see Michelsen and Nocke 1974; Michelsen 1979), vertebrates such as frogs (Chung et al. 1978; Pettigrew et al. 1978) and birds (Coles et al. 1980; Hill et al. 1980; Lewis and Coles 1980). Briefly, the pressure gradient depends on the simultaneous action of sound waves incident to both sides of a membrane. When the sound pressures are closely matched, the net driving force or pressure acting on the membrane will depend on the relative phase of the two waves. Since the phase difference depends on the length of the sound path to each side of the membrane, the acoustical interaction can be highly sensitive to direction. Pressure gradient receivers may occur when two tympana

are acoustically coupled by an air-filled cavity or tube, so that there is a directionally dependent phase shift between the external and internal pressures at each tympanum (Fletcher and Thwaites 1979; Michelsen 1979). In birds, pneumatization of the skull has led to the formation of an interaural canal or cavity directly connecting the two middle ear cavities (Wada 1923). Of crucial interest to directional hearing in owls is the fact that their interaural canals are the largest and most patent of all birds (Tiedemann 1810; Stresemann 1934; Payne 1971; Norberg 1978; Coles, unpublished observations). Therefore it is reasonable to expect the owl ear to be sensitive to a pressure gradient, despite negative findings so far (Schwartzkopff 1962; Payne 1971; Moiseff and Konishi 1981b).

The present study examines the acoustical and directional properties of the external ear of the barn owl by measuring sound pressure in the ear canal and outer ear cavity. In addition, the directional sensitivity of the ear is determined by recording the cochlear microphonic (CM) potentials. The results are compared from both recording techniques and suggest a physical mechanism of directional hearing, based on the combined effects of sound diffraction by the outer ear cavity and a pressure gradient at the TM.

Materials and methods

Subjects and preparation. A total of 6 adult barn owls (*Tyto alba*) were used for measurements of sound pressure in the external ear and recordings of CM potentials. Anaesthesia was produced in the owls (average mass 375 g) by sub-cutaneous injection of a mixture of Ketamine (20 mg/kg) and Rompun (2.5 mg/kg) and maintained by supplementary injections of these drugs. The head was held by a small metal post attached to the dorsal skull with dental cement and connected to an adjustable ball joint. Access to the round window of the cochlea was made by boring a small hole in the ventro-medial skull, medial to the tympanic ring on each side of the head. Insulated silver wires (0.3 mm) with bare ends were implanted bilaterally, touching the surface of the round window membrane; an indifferent electrode was attached to the dorsal neck musculature. After visually positioning the silver wire electrodes, the holes in the skull were sealed with dental cement. Physiological recordings were terminated by sacrificing the animal with a drug overdose and without altering the head position, small microphones (1/4" Brüel & Kjaer Type 4135) were implanted into the side wall of each ear canal adjacent to the outside surface of the TM (Fig. 1B). For additional sound pressure measurements, a microphone (1/8" Brüel & Kjaer Type 4138) was placed in the outer ear cavity at the entrance to the ear canal, by inserting it through the facial ruff feathers from the rear (Fig. 1B).

Stimuli and recordings. Each owl was placed in the centre of an anechoic room (2.6 × 2.5 × 2.0 m) and supported by a small platform out of the frontal sound field. For measurements of sound pressure, pure tones were generated by an oscillator

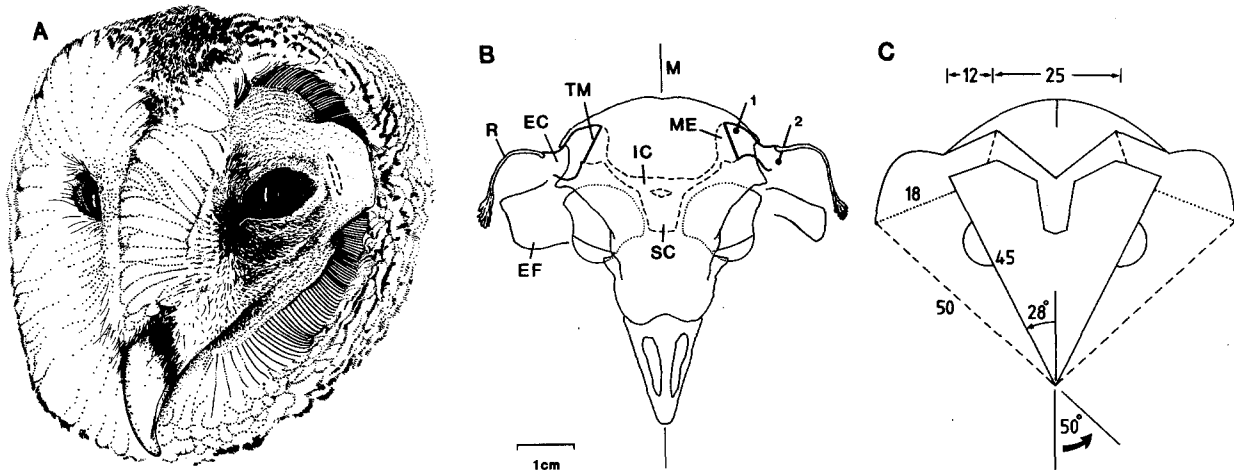


Fig. 1. **A** Head of the barn owl (*Tyto alba*) with facial disk feathers removed, revealing the left outer ear cavity as viewed from the acoustic horizon. Tips of facial ruff feathers form the open face or aperture of the cavity. Position of left ear canal opening (dashed outline) is obscured by the pre-aural flap, and higher than the right ear canal opening. **B** Dorsal view of the barn owl skull showing relevant features of the peripheral auditory system. Plane of section approximately through acoustic horizon (see text for definition). *EC* ear canal and *EF* pre-aural (ear) flap (note left-right asymmetry); *IC* interaural cavity or canal; *M* midline sagittal plane; *ME* middle ear cavity; *R* profile of facial ruff feathers; *SC* sphenoid sinus cavity of the basisphenoid bone; *TM* tympanic membrane; 1, position of microphone in ear canal. 2, position of microphone in outer ear cavity, at entrance to ear canal. For further details see Payne (1971), Norberg (1977). **C** Highly schematic cross-section of the barn owl head, taken from **B**. Dimensions of the asymmetrical outer ear cavity, relevant to the calculation of movement of the acoustic axis in azimuth arc (see text, Fig. 7A): diameter of opening to the cavity (50 mm) and inclination of plane of opening to the midline (50°); diameter of the cavity at the approximate normal truncation point (18 mm); internal length of the extended edge of the cavity (45 mm) and angle to the midline (28°). Dimensions of the internal head cavities are: average length of ear canal (12 mm), see also Table 1; interaural TM distance through the interaural canal (25 mm)

(Hewlett-Packard Model 3300A) and connected to an amplifier (Pioneer BP-320) via an attenuator (Hatfield Type 2125). The amplified signal was connected to a loudspeaker (Motorola piezohorn KSN 1025A for frequencies 1.5–16 kHz or a Clarian electrodynamic speaker for frequencies 0.4–2.0 kHz). Either transducer was mounted on a trolley and attached to a vertical semi-circular aluminium arc (diameter 94 cm). This arc was pivoted at the floor and ceiling of the anechoic room and rotated by a remotely controlled motor at the base. The trolley carrying the loudspeaker was pulled along the arc by a second motor enabling the sound source to be positioned with an accuracy of $\pm 0.5^\circ$ in azimuth and elevation. In each preparation, the owl head was photographed in the standard planes of the sound delivery apparatus to relate head orientation to the spatial coordinate system.

Electrical recordings of CM potentials were amplified (Tektronix FM 122 pre-amplifier) and displayed on an oscilloscope screen. The root-mean-square (RMS) voltages of undistorted CM waveforms were determined by a narrowband (6 Hz) wave analyzer (Marconi) which also provided the signal source. CM amplitude was converted to changes in sensitivity to sound pressure, using a source positioned at the CM axis to produce the maximum voltage for each test frequency. The output voltage from the microphones was measured in dB as sound pressure level (SPL) re. 20 μ Pa by a measuring amplifier (Brüel & Kjaer Type 2510; linear 2 Hz–200 kHz) via a Krohn-Hite filter (Model 3220; high-pass 100 Hz).

To study directionality, both CM potentials and sound pressure in the external ear were plotted on a zenithal projection of the frontal hemisphere (see Figs. 3 and 8). This projection is approximately equal area (distortion of solid angle $< 5\%$) for positions greater than about 30° from the poles. At each test frequency, data points were plotted as iso-pressure or iso-sensitivity contours, by connecting sound source locations pro-

ducing equal sound pressure or CM amplitude respectively, relative to the maximum value at the axis (for definitions see below). The free field sound pressure was calibrated by a reference microphone (1/4" Brüel & Kjaer Type 4135) positioned at the centre of the head, without the owl present, and facing the loudspeaker along the longitudinal axis (0° azimuth, 0° elevation).

Results

Structure of the external ear and interaural canal

Externally, the face of the barn owl is two flat facial discs which meet over the beak at an angle of about 50° to the midline (Fig. 1). When the feathers of the facial disc are removed, several rows of specialized densely-packed feathers are revealed which form the facial ruff (Fig. 1A; Payne 1971). The cavity formed by the side of the head and curvature of the ruff feathers is defined as the *outer ear cavity* (Norberg 1977). The left and right pre-aural flaps and the ear openings are similar in size and shape (Payne 1971; Norberg 1977) but bilaterally asymmetrical because they are equally offset from the horizontal plane (Norberg 1977; Knudsen 1980). Anatomically the ear openings lie on an interaural plane inclined about 12° to the horizontal, with the left opening higher than the right (Norberg 1977). The ruff has a curved appearance

and the ear flaps are mutually inclined by about 26° (Fig. 1A, see also Payne 1971). A detailed pterylogical and photographic examination of the owl head reveals that, as far as can be determined, both facial ruffs have left-right symmetry and therefore ear asymmetry in this species is due to the position of the ear canal openings and preaural flaps only.

The TMs of the barn owl are symmetrical about the midline, with an average radius of 4.5 mm, but they terminate the ear canal rather obliquely (Fig. 1B). Behind each TM, an extensive interaural cavity is formed by the connection of the two middle ear cavities and a wide canal (up to 4 mm in width), which itself is connected to a third air chamber at the midline (Fig. 1B; for further details of anatomy see Payne 1971; Norberg 1977).

Acoustic gain of the external ear, facial ruff and outer ear cavity

At each test frequency, the speaker was positioned at the *acoustic axis* of the external ear which produces the maximum sound pressure in the ear canal (see below). Axial sound pressures were then compared to the free field pressure to estimate the acoustic gain of the external ear (Fig. 2A). The results show that in the intact external ear, no significant pressure gain occurs below about 0.8 kHz but for higher frequencies there is increasing amplification reaching a peak of about 20 dB between 3–9 kHz. The gain measured in the ear canal decreases sharply to about 6 dB above the free field at frequencies up to 15 kHz. After collecting normal gain curves, the entire facial ruff and lore feathers were cut off and the residual gain curve is shown in Fig. 2A, indicating a general decrease in sound pressure in the ear canal between 1–10 kHz compared to normal. With the ruff removed, pressure gain in the ear canal progressively increases to about 12 dB near 10 kHz and typically several small peaks are seen. Above 11 kHz pressure gain in the ear canal drops sharply, remaining similar to the gain in the intact external ear.

The gain of the facial ruff can be estimated by the difference between intact and ruff-removed conditions (Fig. 2A). The amplifying effect of the ruff gradually increases to a peak of around 12 dB in the range 5–8 kHz. Above 8 kHz, the pressure gain produced by the ruff decreases rapidly to about 0 dB near 15 kHz.

Measurements of sound pressure within the outer ear cavity itself, at the entrance to the ear canal, are shown in Fig. 2B. Pressure amplification

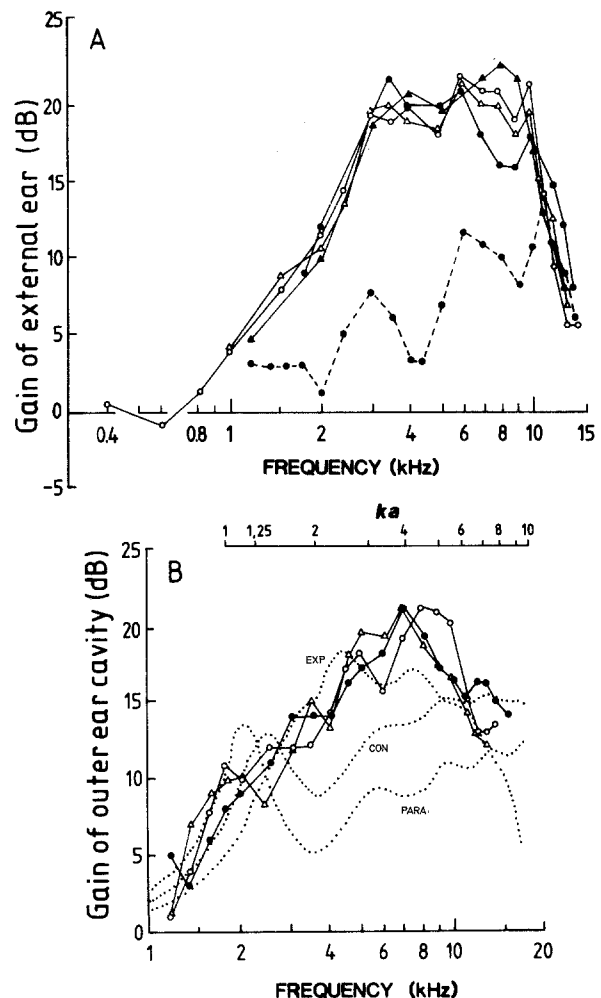


Fig. 2. **A** Acoustic gain of the external ear of the barn owl ($n=4$) obtained from pressure measurements in the ear canal relative to the free field pressure (see Fig. 1B). Sound source positioned at the acoustic axis (for definition see text and Figs. 3, 7) for each test frequency. Dashed line is gain after removal of the facial ruff feathers for a single ear. **B** Acoustic gain of the outer ear cavity ($n=3$) obtained by pressure measurements in the cavity at the entrance to the ear canal (see Fig. 1B). Details as in A. Dotted curves are expected gain for a finite-length paraboloidal (PARA), conical (CON) and exponential (EXP) horn of equivalent dimensions to the outer ear cavity (see Table 1). For methods of calculation see text, also Coles and Guppy (1986), Guppy and Coles (1988). Upper abscissa expresses the circumference ($2\pi a$) of the cavity (horn) mouth as a proportion of the wavelength (λ) i.e. $2\pi a/\lambda$ or ka (see Beranek 1954)

follows a similar trend to the ear canal measurements for the intact cavity (compare Fig. 2A) but gain measured in the ear canal is slightly augmented in the range 2.5–4.5 kHz and near 6 kHz. Also, gain in the outer ear cavity remains slightly higher above 10 kHz compared to the ear canal measurements where pressure gain is rapidly attenuated.

The outer ear cavity can be treated as a horn-

Table 1. Physical dimensions (mm) of the external ear of the barn owl ($n=4$) measurements are means with standard error (brackets)

Outer ear cavity							Ear canal
Mouth ^a			Throat ^b	Length ^c			Length ^d
Height	Width	Radius	Radius	Long	Short	Average	Average
70 (2.0)	45 (2.1)	30 (1.9)	4 (0.4)	70 (1.9)	18 (1.7)	44 (1.8)	12 (1.0)

^a Based on the open face of the facial ruff (see Fig. 1A), average radius is calculated from the measured perimeter

^b Average radius at opening to ear canal (see Fig. 1A, B)

^c Outer ear cavity is extremely asymmetrical in cross-section; acoustical path length of the (horn) cavity is taken as the metrical average from the longest and shortest sides of the cavity (see Fig. 1A, B)

^d Entrance of ear canal to tip of manubrium. Ear canals are asymmetrical due to position of opening and terminated obliquely by the tympanic membrane (Fig. 1B)

like sound receiver in a similar fashion to the mammalian pinna (Coles and Guppy 1986). It is important to note that removal of the facial ruff in the barn owl is a less complete procedure than removal of the pinna (Coles and Guppy 1986; Guppy and Coles 1988) because a significant part of the internal surface of the outer ear cavity involves the face. Therefore the gain of the outer ear cavity is best estimated by a microphone positioned at the entrance to the ear canal (throat) with the external ear intact (Fig. 1B). The horn mouth is created by the open face of the ruff with an average radius determined by the perimeter of the ruff feather tips (Fig. 1A; Table 1). The throat of such a horn is formed at the entrance to the ear canal (ear opening), created by a very abrupt transition between the outer ear cavity and the ear canal (Fig. 1B). Since the outer ear cavity is not symmetrical, the length of the horn is estimated, for simplicity, as the average distance from the throat to the longest and shortest sides of the mouth (Table 1). The gain of the outer ear cavity can be compared to a simple acoustic horn and expected gain can be calculated from the expressions given by Olson (1947) using the methods of Fletcher and Thwaites (1979), as applied to the mammalian pinna (Coles and Guppy 1986; Guppy and Coles 1988). The expected excess pressure at the throat of a finite-length paraboloidal, conical and exponential horn has been plotted for comparison with the experimental data (Fig. 2B). The average gain curve of the outer ear cavity is probably closest to an exponential horn up to about 15 kHz. The excess pressure at the throat (ear opening) would be expected to reach a maximum of 18 dB (excluding resonance) based on the ratio of mouth to throat cross-sectional areas (see Table 1) and is consistent with the observed gain peaks between 5–8 kHz (Fig. 2B).

Ear flap removal was found to alter the sound pressure in the ear canal by a maximum of only 4 dB in the range 2–14 kHz and the effects were not systematic with frequency. The ear flaps were moved manually to see if there was any effect on sound pressure in the ear canal. Pushing the flap as far forward as possible or back towards the ruff changed the sound pressure by only 3 dB for frequencies up to 10 kHz.

Directional sensitivity of the external ear

Directivity patterns. Above 2.5 kHz, directivity patterns based on sound pressure measured in the ear canal, show a major lobe with a region of maximum pressure called the *acoustic axis*. A typical series of directivity patterns for the left and right external ears are shown in Fig. 3 for frequencies between 3–9 kHz. Higher frequencies produce a more directional pattern in general, as seen by the closeness of the contour lines. However, the isopressure contours of the major lobe tend to elongate in the horizontal plane at high frequencies, particularly towards the midline. Above 5 kHz in the frontal hemisphere, the major lobe is bordered by troughs of low pressure causing secondary lobes in the directivity pattern. These low pressure regions contain extreme minima or approximate nulls, forming crescents around the major lobe.

The frequency dependence of directionality was quantified by measuring the difference between the maximum pressure on axis and the minimum pressure at the null in individual directivity patterns (Fig. 4A). The results show that the external ear becomes directionally sensitive above about 3 kHz and highly directional above 6 kHz, largely as a result of the increase in amplification (Fig. 2A) and the development of nulls in the directivity patterns (see below and Fig. 3).

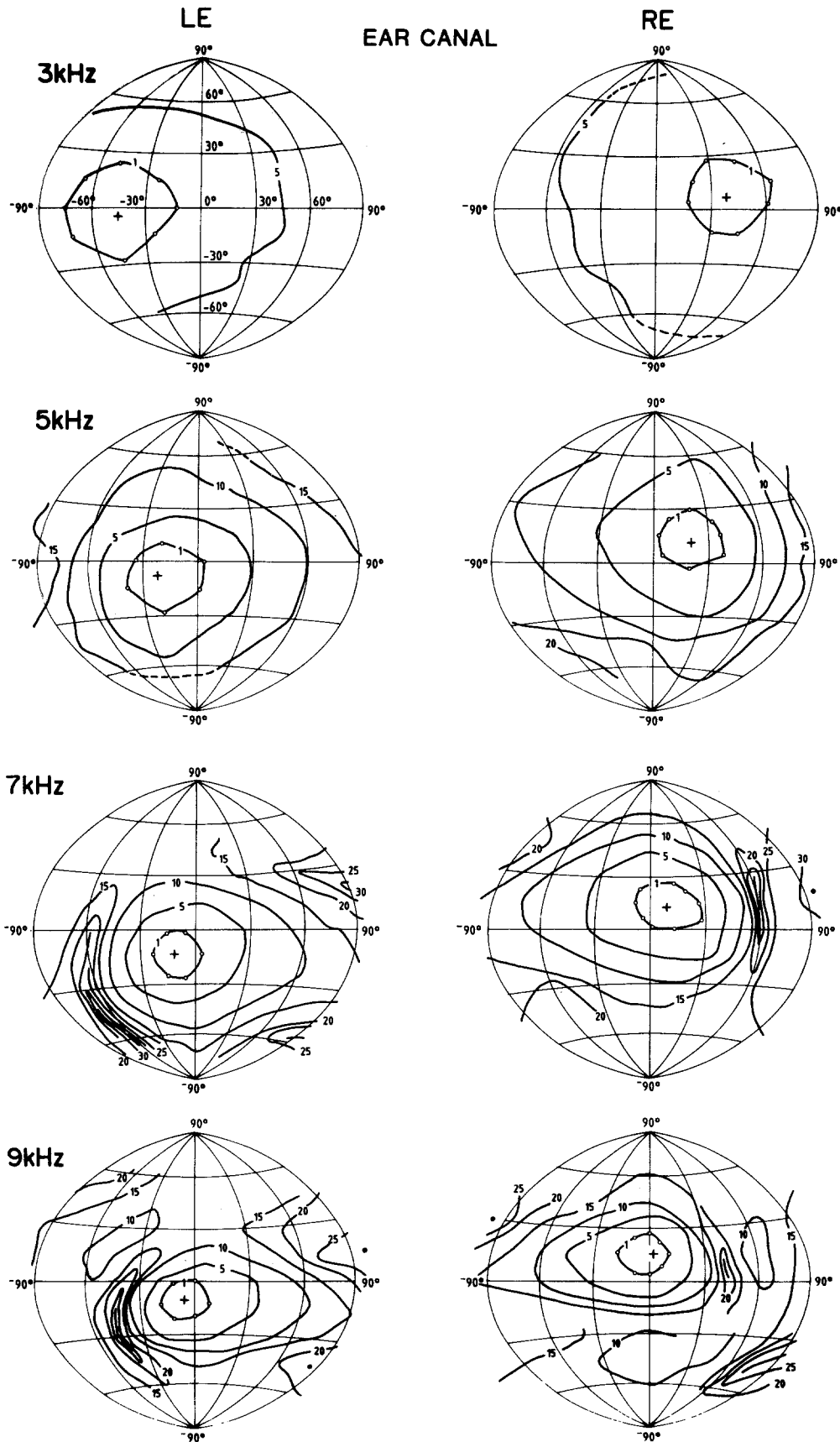


Fig. 3. Directivity patterns for the external ear of the barn owl (test frequency indicated), based on pressure measured in the left and right ear canal of the same owl. Contour lines represent speaker locations of equal pressure, for decreases in pressure (dB) relative to the maximum at the acoustic axis (cross within -1 dB contour). Null positions indicated by filled circle or line, usually below the -30 dB level. Projection of frontal hemisphere is zenithal and equal area for positions greater than 30° from the poles (for details see Materials and methods). By convention, the owl's right is to the right of the vertical plane at 0° azimuth

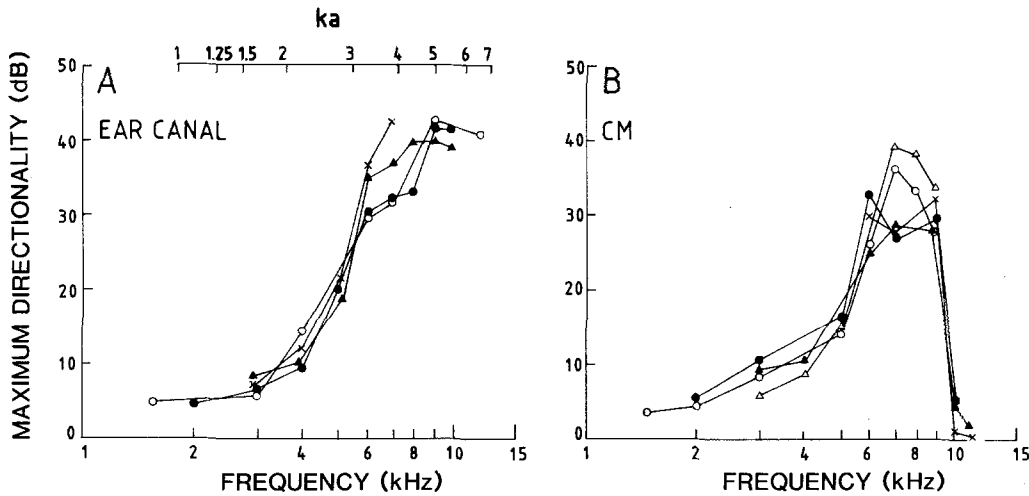


Fig. 4. **A** Difference between the maximum (at the acoustic axis) and minimum (or null) sound pressure for individual directivity patterns of the external ear in the barn owl ($n=4$). Derived from directivity patterns as shown in Fig. 3. Upper abscissa expresses the circumference of the mouth of the outer ear cavity relative to the wavelength or ka . **B** Difference between the maximum (at the axis) and minimum (null) CM amplitude, estimated from individual CM directivity patterns (see Fig. 8) in the barn owl ($n=5$). Note the rapid loss of CM directivity above 9 kHz

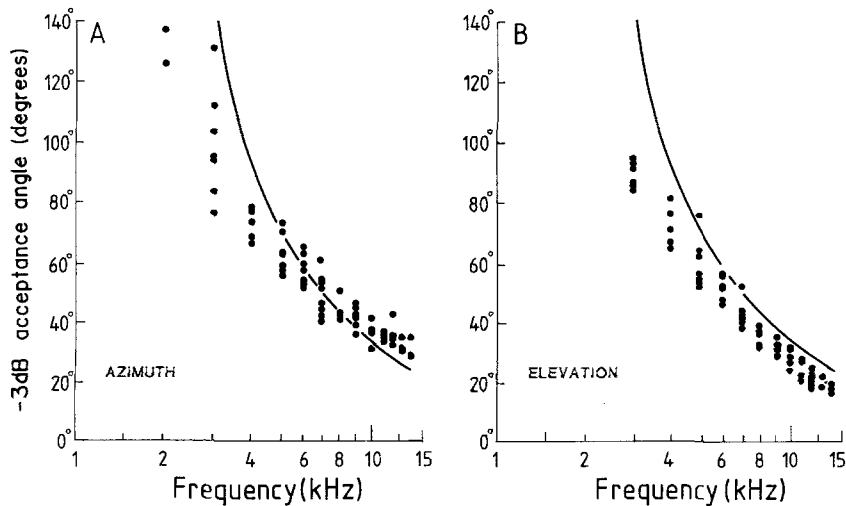


Fig. 5. **A, B.** Measurements of the -3 dB acceptance angle (relative to the acoustic axis) for the major lobe of directivity patterns for the external ear. Acceptance angles are estimated at the full angular width of the azimuth (**A**) and elevation (**B**) boundaries of the -3 dB contour (see Fig. 3). Solid curve is the expected -3 dB acceptance angle for sound diffraction by a circular aperture, with an average radius equal to the open face (mouth) of the outer ear cavity, formed by the facial ruff (Table 1; Fig. 1A). For details of calculation see text and Coles and Guppy (1986). Note that the expected curve is the full angular width (2θ) of the major lobe, normally expressed as the half width (θ) in physical systems (Beranek 1954)

Directivity of the major lobe. The angular width or acceptance angle of the major lobe of directivity patterns was estimated at the -3 dB contour, relative to the axial pressure, for each test frequency (see Coles and Guppy 1986). Acceptance angles were plotted separately for azimuth and elevation (Fig. 5A, B) to show the asymmetry of the major lobe (Fig. 3). The results indicate that as frequency increases from 2–14 kHz, acceptance angles systematically decrease from about 130° to 30° in azimuth and 90° to 18° in elevation.

The experimental data in Fig. 5 were compared with diffraction theory (Beranek 1954) by treating the open face of the outer ear cavity, for simplicity, as a single circular aperture. A similar approach has been applied to the directional properties of

the mammalian pinna (Coles and Guppy 1986; Guppy and Coles 1988). The aperture of the outer ear cavity is delineated by the tips of the ruff feathers and the lore (Fig. 1A) as used in calculation of horn gain (see above, Fig. 2). The expected curves in Fig. 5 are based on the -3 dB acceptance angle for a circular aperture of the same radius as the mouth of the outer ear cavity (Table 1). Generally, there is a good fit to the experimental data, particularly in azimuth for frequencies between 5–10 kHz (Fig. 5A).

Nulls. In frontal space and above 5 kHz, regions of low pressure forming deep troughs or nulls were a prominent feature for directivity patterns of the external ear. The spatial gradient (sharpness) of

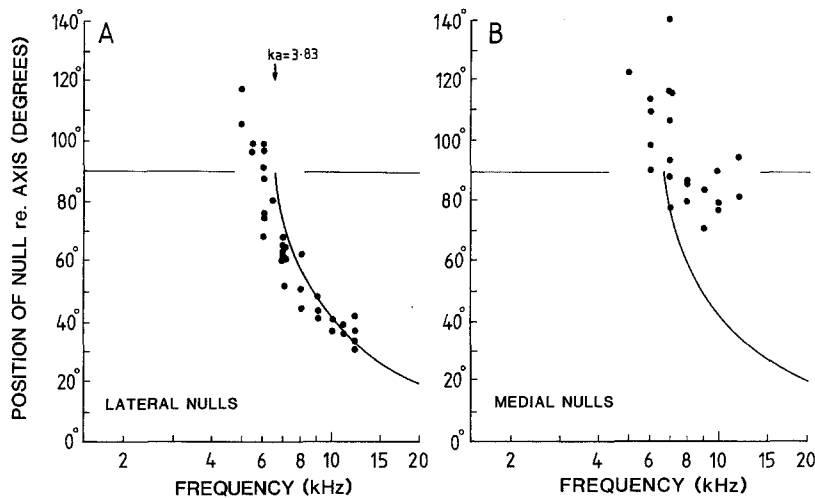


Fig. 6A, B. Angular separation between nulls and the acoustic axis, estimated from directivity patterns of the external ear in the barn owl as shown in Fig. 3. Solid curve is the expected angle between the acoustic axis and the first null (semi-angle), which forms the major lobe resulting from sound diffraction by a circular aperture. Radius of the mouth of the aperture based on the open face of the outer ear cavity (Table 1). Horizontal line at 90° represents the theoretical limit of diffraction nulls in frontal space for a baffled aperture; vertical arrow ($ka=3.83$) indicates the low frequency limit (7 kHz) for diffraction nulls occurring 90° from the axis, for a circular aperture with the average radius of the mouth of the outer ear cavity (Table 1)

the major lobe was clearly influenced by the angle separating the acoustic axis and nulls. This relationship was quantified as shown in Fig. 6A for the most extensive null regions located in the lateral quadrants, relative to the acoustic axis (ipsilaterally) of each ear (see Fig. 3). However medially positioned nulls (Fig. 6B), located in contralateral space, were more difficult to determine, due to the progressive elongation of the main lobe in azimuth at high frequencies (Fig. 3). Nulls lateral to the acoustic axis moved closer to the axis from about 100° down to 30° as frequency increased from 5–12 kHz (Fig. 6A). In contrast, the angular separation between medial nulls and the acoustic axis exceeded 70° (Fig. 6B), emphasizing a much poorer spatial gradient due to the asymmetry of the major lobe in azimuth.

Diffraction theory predicts nulls in the directivity patterns of a circular aperture (Beranek 1954) but nulls are limited to frontal space for a baffled opening. Thus the expected semi-angle of the major lobe, created by the first diffraction null, is plotted in Fig. 6 for comparison with the experimental data, based on the average radius of the mouth of the outer ear cavity (Table 1; for method of calculation see Coles and Guppy 1986). The observed semi-angles for laterally placed nulls (Fig. 6A) are close to expected values but angles between the acoustic axis and medial null regions (Fig. 6B) are not explained by a diffraction model for a circular aperture. Here the asymmetry of the mouth of the outer ear cavity may need to be considered (see Coles and Guppy 1986). Nulls lying behind the plane of opening of the outer ear cavity ($>90^\circ$, Fig. 6) may be explained by the diffraction properties of an aperture at the end of a long pipe rather than an infinite baffle (Beranek 1954; Coles and Guppy 1986).

Bilateral asymmetry of directivity patterns. Directivity patterns of the external ear are clearly asymmetrical, both unilaterally and bilaterally (Fig. 3). Nevertheless, at a given frequency, the directivity of each external ear is an inverted pattern of the other, since patterns can be superimposed after 180° rotation about the longitudinal axis. When the midline sagittal plane of the barn owl head is aligned to the vertical plane of the sound delivery apparatus, there is a disparity in elevation between the directivity patterns of the left and right external ears (Fig. 3). The average positions of the acoustic axes are $\pm 6^\circ$ from the horizontal plane for frequencies below 4 kHz (Fig. 7B). Between 5–10 kHz, as the patterns become more directional, the vertical disparity increases to an average of 26° remaining relatively independent of frequency, with the right ear acoustic axis higher than the left. The *acoustic horizon* is defined by the plane where the acoustic axes are equally offset in elevation i.e. $\pm 13^\circ$ for the right and left ear respectively. This acoustical disparity is correlated with the anatomical asymmetry of the ear openings – the ear flaps are symmetrically placed over the entrance to each ear canal but the mutual angle between the surfaces of the ear flaps is about 26° . Therefore the acoustic horizon corresponds to a plane bisecting the two planes perpendicular to the surface of each ear flap. It follows that the acoustic axis will be below and above the horizon for the left and right ears respectively, despite the appearance of the left ear opening to be higher than the right (Payne 1971).

Frequency shift of the acoustic axis. The directivity patterns illustrated in Fig. 3 indicate that the acoustic axes of the external ear move towards the midline at higher frequencies. In azimuth, the axes

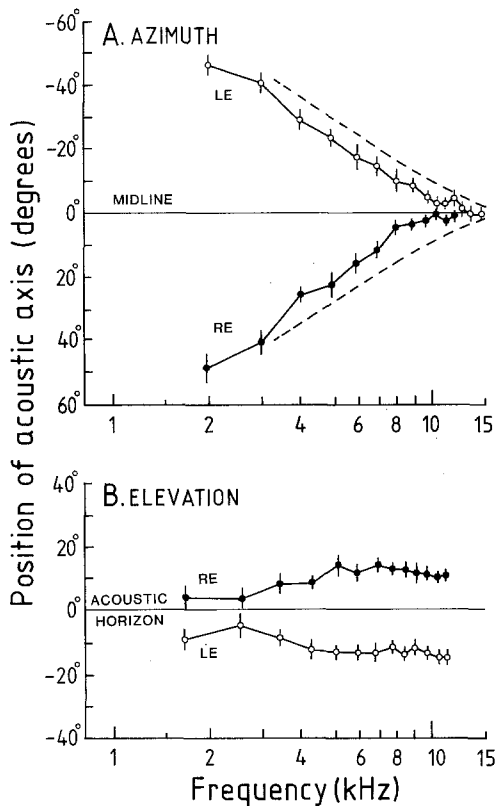


Fig. 7. **A** Average position of the acoustic axis in azimuth, relative to the midline, for four left (*LE*) and right (*RE*) external ears of the barn owl derived from directivity patterns as shown in Fig. 3. Vertical bars at each data point are standard error. Dashed lines are the expected movement of the acoustic axis resulting from sound diffraction by an obliquely truncated horn, based on the asymmetry of cross-section of the outer ear cavity (Fig. 1B, C). For details of calculation see text and Guppy and Coles (1988). **B** Average position of the acoustic axis in elevation, details as in A. Axis position is relative to the acoustic horizon (for definition see text)

start about 50° ipsilateral to the midline at 2 kHz and move symmetrically at a rate of about 20°/octave up to 10 kHz (Fig. 7A). At higher frequencies both axes remain ipsilateral and within 5° of the midline.

It is possible to predict the movement of the acoustic axis in azimuth resulting from the asymmetry of the facial ruff, if the outer ear cavity is regarded as an obliquely truncated horn (Guppy and Coles 1988). The wave fronts travelling towards the throat from the longer sides will be delayed relative to the shorter sides. The significance of this delay becomes apparent when the phase shift exceeds 180° because the wave energy originating from the longer paths will start to subtract energy and so reduce the signal. Based on the geometry of the outer ear cavity (Fig. 1C), the expected azimuthal position of the acoustic axis has been calculated using the method of Guppy and

Coles (1988) and the results are plotted in Fig. 7A. The expected values are in good agreement to the experimental data and both the predicted and observed movement for the acoustic axis are about 20°/octave. Both axes are approximately normal to the plane of opening of the facial ruff at low frequencies (Fig. 1).

Removal of the facial ruff and pre-aural flap. Removal of the facial ruff was found to substantially reduce the directional properties of the external ear as well as the vertical asymmetry between the directivity patterns of the two external ears. Loss of directionality was characterized by considerable expansion and irregularity of the iso-pressure contours, generally resulting in less than 10 dB change in sound pressure over the entire frontal hemisphere, even at high frequencies. Null regions disappeared following ruff removal and were replaced by regions with a very low spatial gradient.

Removal of the ear flap, moving it forwards or backwards produced no gross changes in directionality and did not alter the position of the acoustic axis or nulls, up to 10 kHz.

Directional sensitivity of the cochlear microphonic (CM)

Directivity patterns. Significant directional sensitivity for the CM became evident above about 2 kHz and the region of maximum amplitude was defined as the *CM axis* (Fig. 8). As for the directivity patterns of the external ear (Fig. 3), the major lobe of CM directivity is depicted by a series of iso-sensitivity contours, in dB relative to the maximum (RMS) amplitude at the CM axis (Fig. 8). The increase in CM directionality as a function of frequency is plotted in Fig. 4B, in a similar fashion to the pressure measurements (Fig. 4A). However, unlike the directionality of the external ear, the CM became rapidly non-directional above 9 kHz, restricting useful directional information to a frequency band between 2–9 kHz.

For frequencies below about 5.5 kHz, CM directivity patterns comprise a series of concentric elliptical-type contours (Fig. 8). Above 5.5 kHz, CM directivity patterns (Fig. 8) are clearly distinct from those of the external ear because the major lobe is flattened (cf. Fig. 3). Spatially, the high amplitude CM response expands into an elongated zone of low directionality containing the CM axis. Individual directivity patterns appear as a diagonal or tilted band of high amplitude extending up to 90° either side of the CM axis, e.g. 7 kHz (Fig. 8).

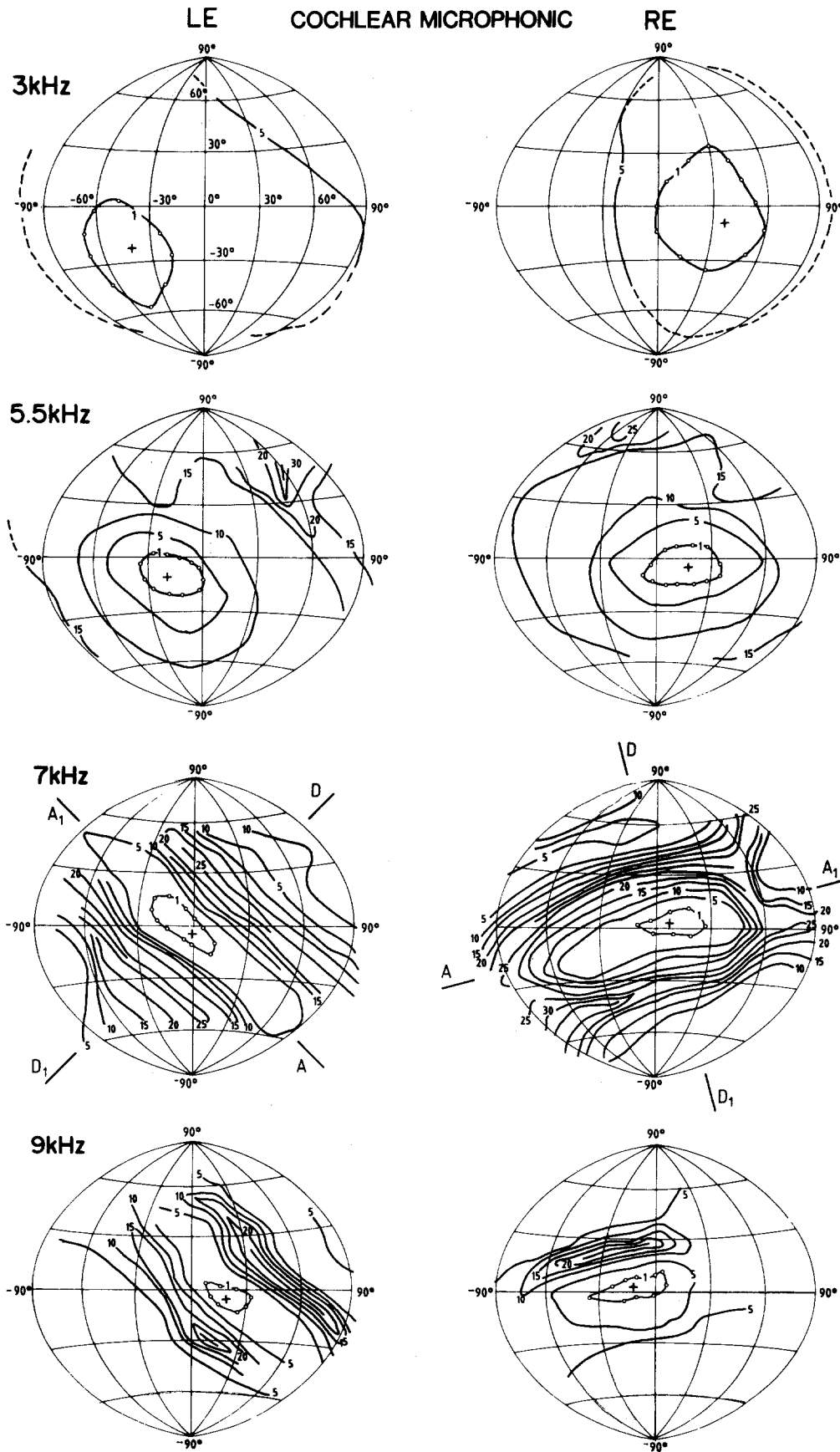


Fig. 8. CM directivity patterns recorded from the left (*LE*) and right (*RE*) ear in a single barn owl. Details of data presentation as in Fig. 3, except contour lines are iso-amplitude CM potentials expressed as equal sensitivity to sound pressure in dB, relative to the maximum amplitude at the CM axis (cross within -1 dB contour). Nulls are represented as troughs of minimum CM amplitude (line), usually 25 dB or more below the peak. The CM axial and directional planes are indicated as AA_1 , and DD_1 , respectively, for directivity patterns at 7 kHz (for definitions see text)

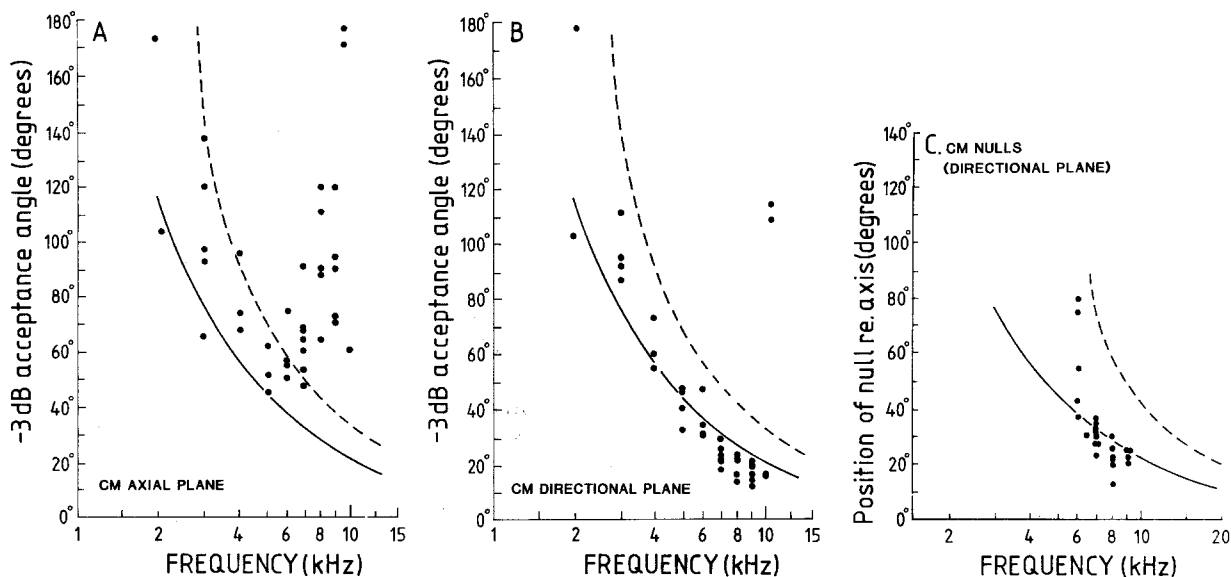


Fig. 9 A, B. Angular width (acceptance angle) of the major lobe of CM directivity patterns, estimated at the -3 dB level relative to the maximum amplitude at the CM axis (see Fig. 8), for the plane of lowest directionality (*CM axial plane*, A) and highest directionality (*CM directional plane*, B). For definition of these planes see text and Fig. 8. Compare with -3 dB acceptance angles for the external ear in Fig. 5. In B, note rapid loss of directionality at 11 kHz. C Position of nulls in CM directivity patterns relative to the CM axis, estimated along the CM directional plane. — In A and B, solid lines are expected angular width of the major lobe, for a 3 dB decrease in the net pressure at the TM relative to the maximum net pressure, resulting from a pressure gradient. In C, solid curve is the expected angular separation between the maximum and minimum net pressures acting on the TM. In each case, calculations are based on the external and internal sound paths to the TM (Fig. 1B, C), for details see text. Dashed curves are expected -3 dB acceptance angles (A, B) and semi-angles (C) for sound diffraction by a circular aperture (see Fig. 5)

These bands are bordered by extensive troughs of low CM amplitude or nulls, running approximately parallel to the band, creating secondary lobes. Thus the major lobe is polarized into an 'axial' plane of very low directivity (*CM axial plane*) and a second, approximately perpendicular plane, of very high directivity (*CM directional plane*). The orientation of these planes is shown in Fig. 8 for directivity patterns at 7 kHz of the left and right ears. The axial planes are orientated about 45° and 75° to the vertical for the left and right ear, respectively, and approximately symmetrical about the *interaural midline*, which is rotated by 12° to the right relative to the midline sagittal plane of the head due to ear asymmetry (Payne 1971).

Directivity of the major lobe. The acceptance angle of the CM major lobe was measured at the -3 dB level (using the iso-sensitivity contour) relative to the maximum amplitude at the axis, for both the axial and directional planes. The results for the CM axial plane are shown in Fig. 9A and the -3 dB acceptance angle decreases from about 180° down to 45° as frequency increases from 2 kHz to 6 kHz. Above 6 kHz, the -3 dB acceptance angle starts to increase rapidly as the CM loses directionality in this plane. Meanwhile, in the di-

rectional plane (Fig. 9B) the -3 dB acceptance angle above 5 kHz is as much as 20° smaller, compared to the directivity of the external ear (Fig. 5) reflecting a narrower, more directional major lobe for the CM. The CM -3 dB acceptance angles reach a minimum of 10° – 20° near 9 kHz. Above 9 kHz, the distinction between a CM axial and directional plane is weakened by the rapid loss of directionality, as indicated by a 90° increase in the -3 dB acceptance angle above 10 kHz (Fig. 9B).

Nulls. The regions of extremely low CM amplitude bordering the CM axis contribute to a very steep spatial gradient along the CM directional plane (e.g. Fig. 8, 7 kHz). The angular separation of nulls from the CM axis was measured along the directional plane, in a similar fashion to the semi-angle of external ear directivity patterns (Fig. 6). The results are shown in Fig. 9C, indicating that CM nulls in the frontal hemisphere occurred between 6–9 kHz only and generally within 15° – 30° of the CM axial plane. Therefore these nulls are about 25° closer to the CM axis compared to the acoustic axis, except for frequencies near 6 kHz (cf. Fig. 6A). This result, together with the -3 dB acceptance angle, indicate that the CM major lobe is significantly sharper in the directional plane be-

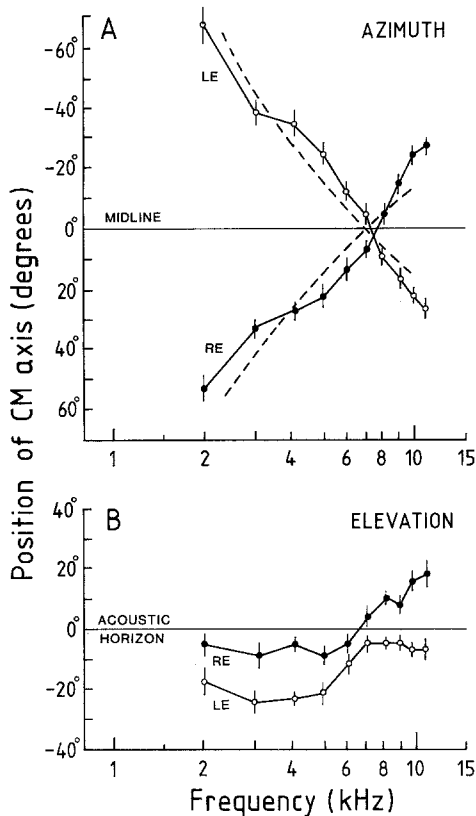


Fig. 10. A Average azimuthal position of the CM axis, relative to the midline, for four left (*LE*) and right (*RE*) ears in the barn owl taken from directivity patterns as shown in Fig. 8. Vertical bars at each data point are standard error. Dashed curves are expected position of the maximum net pressure acting on the TM due to a pressure gradient and resulting from the external and internal sound paths to the TM in the barn owl (for details see text and Fig. 1B, C). Note that the expected maxima cross at the midline near 7 kHz as a result of the phase delay through the interaural cavity at this frequency. Compare with the movement of the acoustic axis (Fig. 7A). B Average position of the CM axis in elevation, details as in A. CM axis positions are relative to the acoustic horizon. Compare with acoustic axis position in elevation (Fig. 7B)

tween 6–9 kHz compared to the directivity of the external ear.

Frequency shift of the CM axis. CM directivity patterns tended to move upwards and towards the midline at higher frequencies (Fig. 8) and these effects are summarized in Fig. 10. In elevation, both CM axes are located below the acoustic horizon between 2–5 kHz (Fig. 10B), with the right ear CM axis being higher by an average of 13°. The right ear CM axis crosses the acoustic horizon between 6–7 kHz and is located about 15° above the horizon at 10 kHz whereas the left ear CM axis remains about 5° below the horizon from 7–10 kHz. In azimuth (Fig. 10A), both CM axes approach the midline at an average rate of 37°/octave

crossing the midline at frequencies near 7 kHz and continuing into contralateral space as frequency increases.

Ear canal blocking. To test for the possibility of sound transmission through the interaural canal, the ear canal was blocked with silicone rubber cement. Ipsilaterally, the effect of blocking decreased the maximum amplitude of the CM by 4–15 dB between 5–8 kHz. Significant effects from blocking the contralateral ear were demonstrated when silicone rubber was used to fill the entire ear canal. The results of such a procedure are shown in Fig. 11 for the left ear CM at 6 kHz and 8 kHz. The main effect of blocking the contralateral ear canal was to change some of the nulls into localized regions of higher CM amplitude or to create new regions of low amplitude. Overall, the major lobe of the CM was relatively undisturbed but some broadening of the major lobe was noted, as well as a slight repositioning of the axis.

Pressure gradient effects. In principle, the barn owl's interaural cavity could function as an acoustic waveguide and therefore the path length to each side of the TM will depend on the angle of sound incidence and the length of the cavity, as proposed for other birds (Coles et al. 1980; Hill et al. 1980). The most direct internal sound path between each TM is about 25 mm (Fig. 1C) giving an interaural transmission time of approximately 73 μ s. It is known that the relationship between interaural time disparity and sound direction in azimuth is approximately 2.2 μ s/degree in the barn owl, as measured in the ear canal (Moiseff and Konishi 1981a). Therefore, by combining these two sources of acoustic delay, the net pressure acting on the TM can be calculated, assuming no amplitude losses or additional delays in interaural transmission and that sound travels at a constant velocity. For an ideal pressure gradient receiver, the maximum amplitude of vibration of the TM will be determined by the sound direction which produces a phase shift of $(2n-1)\pi$ between the interacting sound pressures. The interaural time disparity required to produce such a phase shift will be a function of the wavelength, in order to maintain a path length difference of $(2n-1)\lambda/2$ and can be calculated for azimuth angles as shown in Fig. 10A. The expected position of the maximum net pressure moves from 80° ipsilateral to 8° contralateral at an average rate of about 40°/octave, crossing the midline near 7 kHz. The expected results compare favourably with the movement of the CM axis for both ears, in contrast to the movement

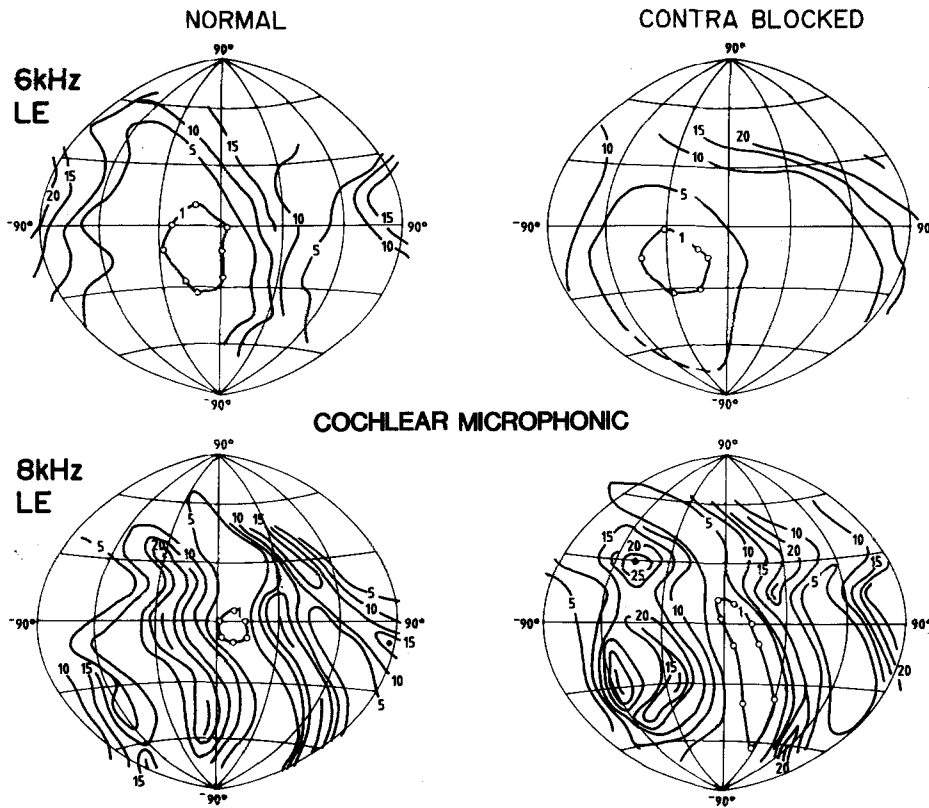


Fig. 11. CM directivity patterns from the left ear of a single barn owl, before (normal) and after (contra blocked) blocking the right (contralateral) ear canal with silicone rubber cement. Details as for Fig. 8

of the acoustic axis (Fig. 7A). The maximum net pressure occurs near the midline at 7 kHz because the internal separation of the two membranes is approximately one half of the wavelength.

Likewise, a 3 dB decrease in the amplitude of the net pressure (relative to the maximum) occurs when the phase difference across the membrane is $(2n-1)\pi/2$, i.e., a path length difference of $(2n-1)\lambda/4$ as shown in Fig. 9A, B. Above 4 kHz, the observed angular width of the major lobe in the CM directional plane is in good agreement with the expected values, if not slightly more directional than predicted at the higher frequencies. Since the CM is highly directional in a preferred plane above 6 kHz (Fig. 8), the CM acceptance angles reflect a substantial decrease in directionality in the axial plane, compared to that predicted by a pressure gradient (Fig. 9A).

Finally, the angular separation between the maximum and minimum amplitudes of vibration of the membrane will be determined by a change in the phase angle of $n\pi$, resulting in a null when equal amplitude pressure occurs each side of the membrane. Calculation of the expected angular separation between the null and the maximum vibration amplitude (semi-angle) is plotted in Fig. 9C and in the frequency range 6–9 kHz, the

observed CM null positions are very similar to predicted values.

Discussion

The results of this study suggest that the directional properties of the barn owl ear result from the interaction of two independent physical factors, namely sound diffraction experienced by the outer ear cavity and pressure gradients at the TM. Monaural directional sensitivity was measured by the amplitude changes of the CM, which may be explained in terms of the net driving pressure on the TM, contrasting sharply with the directional sensitivity of the external ear (Figs. 3 and 8). In pressure receivers such as the mammalian ear, CM directionality is very similar to the directivity patterns obtained by pressure measurements in the ear canal, resulting from sound diffraction by the pinna (Middlebrooks and Pettigrew 1981; Phillips et al. 1982; Coles and Guppy 1986). Interestingly, both the outer ear cavity of the barn owl and the mammalian pinna have acoustical properties similar to a horn-like receiver (Coles and Guppy 1986; Guppy and Coles 1988) but the barn owl ear, like birds in general, may be sensitive to a pressure gradient and therefore inherently directional.

Since CM directivity patterns support the idea of pressure gradients at the TM, the present results imply functional sound transmission through the interaural cavity (cf. Moiseff and Konishi 1981 b). If this suggestion is correct then the acoustical behaviour of the system may approximate a doublet tube ear (Fletcher and Thwaites 1979). It is possible that the interaural cavity may be specifically designed to transmit sound efficiently for a relatively narrow band of frequencies which are known to determine the neural coding of auditory space (Knudsen and Konishi 1978 a, b) and accurate sound localization (Konishi 1973 b; Knudsen and Konishi 1979). In fact, the length of the interaural cavity is approximately half the wavelength of the frequency band most accurately localized by the barn owl and acoustical resonance of the auditory system may be a part of the directional mechanism. The peaks of gain detected by pressure measurements in the ear canal (Fig. 2A) are an approximate harmonic series. Thus the combined length of the ear canal and interaural cavity may resonate as a tube closed at one end, possibly due to stiffening of the contralateral TM under the free field conditions. Clearly further experiments are needed to fully understand the acoustical role of the internal cavities of the barn owl head in directional hearing. Failure of the directional mechanism above 9–10 kHz (Fig. 4B) may be linked to the rapid loss of pressure gain in the ear canal (Fig. 2A).

If the barn owl ear is sensitive to a pressure gradient, then it will control the directional response as long as there is a phase shift across the TM, provided the pressures are closely matched. In a doublet tube ear with symmetrical input ports, the vibration of the membrane will be influenced most by changes in sound direction in the interaural plane. In the barn owl, however, this plane (the interaural axis) is tilted by 12° to the right of the midline of the head because the ear openings are asymmetrical (Payne 1971). Consequently, the planes of equal interaural phase (or time) difference, running parallel to the interaural midline, will be similarly inclined to the midline of the head. Such an effect has been shown in *Aegolius funereus* (Norberg 1968, 1978), but ear asymmetry in this species is opposite to *T. alba* because the right ear opening is higher than the left. In the present study, the axial plane of the major lobe of both left and right ear CM directivity patterns tends to rotate away from the interaural midline for frequencies above 5 kHz but their orientation remains approximately symmetrical about the *interaural midline* (Fig. 8). The onset of this effect occurs rapidly,

co-incident with a highly directional pressure response generated by the outer ear cavity (Fig. 4A).

Sound diffraction

In addition to the possible effects of a pressure gradient at the TM, ear directionality is influenced by sound diffraction at the open face of the outer ear cavity. To a first approximation, directionality of the external ear was found to be related to sound diffraction by a single circular aperture. As for a horn receiver (Beranek 1954), the outer ear cavity generates a directional response above 2 kHz because the wavelength becomes less than the circumference of the opening ($ka > 1$; Fig. 4A). Likewise, the external ear becomes a highly directional receiver above 5 kHz as the wavelength approaches the diameter of the opening ($ka > 3$). It is quite misleading to regard the facial ruff or indeed the entire outer ear cavity as a parabolic reflector, although the ruff resembles a concave sound collecting surface (Fig. 1A; Konishi 1973 a; Knudsen and Konishi 1979; Knudsen 1980). For frequencies audible to the barn owl, the acoustical properties of the outer ear cavity can be adequately described by the physics of sound diffraction at the mouth (Figs. 5 and 6) and pressure transformation by a horn-like external waveguide (Fig. 2B).

Unlike many mammalian pinnae, the outer ear cavities of the barn owl are fixed in relation to the head. However, the shape and mutual orientation of the facial ruffs ensure a considerable overlap between the major lobes of the directivity patterns of the external ear in frontal space (Fig. 3). This overlap may facilitate a pressure gradient at each TM because the sound pressures at the two input ports are closely matched. In order to maintain these conditions, some directionality is sacrificed towards the midline at higher frequencies (but acoustic gain is high, see below), coupled with movement of the directivity pattern towards the front of the head (Fig. 7A). Thus sound diffraction by the outer ear cavity can be seen to place an important spatial limitation on the possibility of a pressure gradient at the membrane. For example, iso-sensitivity contours along the CM axial plane are restricted (Fig. 8), instead of forming bands of high CM amplitude which may be expected to completely encircle the head in a simple doublet tube ear. Presumably these restrictions occur when the sound pressure differs by more than 6 dB or so either side of the TM, depending on diffraction by the outer ear cavity and therefore effectively eliminating a pressure gradient, irrespective of the phase shift (Michelsen and Nocke 1974). Further-

more, sound diffraction by the outer ear cavity is likely to affect the orientation of the CM major lobes in each ear because the interaural equal pressure (intensity) difference (IID) contours rotate anticlockwise with increasing frequency. This is due to the bilateral asymmetry in elevation and the frequency dependent azimuthal position of directivity patterns of the external ears (Figs. 3, 7A; Payne 1971; Knudsen 1980). Movement of the acoustic axis in azimuth seems to result from the asymmetry of the outer ear cavity, as reported for the pinnae of some bat species (Guppy and Coles 1988).

Measurements in the present study show that the vertical disparity between the left and right acoustic axes is actually about 26° , compared to the previous estimates of 10° – 15° in the barn owl (Payne 1971; Knudsen and Konishi 1978 b). The anatomical asymmetry of the external ears in the barn owl appear to govern the position of the acoustic axes in elevation as in other owl species (*Asio otus*, Schwartzkopff 1962; *Aegolius funereus*, Norberg 1968). The reason why such an asymmetry should require the interaural axis to be tilted by about 12° – 13° is not immediately apparent, until the movement of the acoustic axis in azimuth is considered as well. For frequencies most accurately localized, i.e. near 7 kHz, the acoustic axes are approximately 13° from the midline. This means that IID contours close to zero, in the region of frontal space where localization is most accurate, are inclined by 45° to the midline. Such an inclination may be optimal for two fixed horn-like receivers in order to provide good spatial resolution in two dimensions. If this suggestion is correct, then ear asymmetry in owls in general may seek to provide a similar acoustical function, despite considerable variation in the morphology of the outer ear cavity between species (Norberg 1977).

The pre-aural flaps are placed directly in front of the ear openings and in the vertical plane, their surfaces are orientated normal to each acoustic axis. However, movement of the flaps or even complete removal had a negligible effect on pressure gain or directionality of the external ear. This may be explained by the relatively small size of these structures compared to the sound wavelengths audible to the owl. The barn owl ear may be sensitive to small changes in pressure caused by voluntary movement of the flap, since it is under muscular control (Stellbogen 1930), but it is difficult to imagine any systematic effect on directionality. Payne (1971) reported that movement of the ear flap caused a significant effect on sound pressure in the ear canal but he performed the test at 13 kHz only, a frequency which is not localized and

probably inaudible to the barn owl (Konishi 1973a, b; Knudsen and Konishi 1979). Payne (1971) also reported that pushing forward the feather conches (ruff) at 5 kHz altered the directivity pattern, but this effect is expected simply by distortion of the mouth of a horn at a frequency which produces high directionality (Fig. 4A). In fact, there is considerable variation in the design of pre-aural flaps in owls; *Phodilus badius*, a close relative of the barn owl, has no pre-aural skin folds despite a prominent ruff (Norberg 1977). Perhaps the ear flaps have a protective role or possibly reduce wind turbulence near the ear opening. Under natural conditions, most movement of the ear flap and ruff occurs during the transition from sleep to the alert or hunting postures (Payne 1971). In *A. funereus* these structures are reportedly stationary during sound localization (Norberg 1970, 1978).

Previous studies of ear directionality in owls

In the barn owl, Payne (1971) reported that both CM and ear canal measurements produced the same directivity patterns, implying that the ear was a pressure receiver. Likewise in *Asio otus*, Schwartzkopff (1962) concluded that the directionality of both CM and auditory nerve evoked potentials resulted from sound diffraction by the head. In contrast, data from Knudsen and Konishi (1978b) at 6 kHz, indicate that directionality patterns of auditory nerve potentials have sharper peaks and nulls compared to the pressure measurements in the ear canal. Their data therefore support the observations of the present study and suggest the existence of a middle-ear mechanism which modifies directionality, compared to diffraction alone.

In general, an important factor in studying directional hearing in birds may be the method of sound delivery, either by a free field sound source or the artificial presentation of sound to each ear by a closed field system. In the barn owl, experiments using dichotic stimulation (via earphones) suggest that above 3 kHz sound pressure is highly attenuated by the interaural cavity thus preventing a pressure gradient at the membrane (Moiseff and Konishi 1981 b). The apparent interaural transmission 'loss' approaches 60 dB at 7 kHz and is clearly not consistent with the interpretation of ear directionality in the present study. One possibility is that resonance modes may be created in the interaural cavity by unilateral or bilateral closed field sound stimulation, which do not occur under free field conditions. A closed sound field may disrupt

the pressure gradient normally established in the free field, particularly if the acoustical properties of the internal cavities are altered by the presence of the external coupling. For example, dichotic sound stimulation in the chicken shows a 30–35 dB interaural transmission loss which would appear to prohibit a significant pressure gradient at the TM (Rosowski and Saunders 1980). In contrast, in the quail under free field conditions, both CM directionality and measurements of pressure and phase near the TM, are characteristic of a pressure gradient receiver (Coles et al. 1980; Hill et al. 1980).

Ear blocking

CM directionality was significantly affected by blocking the contralateral ear canal suggesting that sound is transmitted through the interaural canal. However, the effects were not as dramatic as demonstrated in the quail, where CM directionality can be eliminated by blocking the contralateral ear canal (Coles et al. 1980). In the present experiments, contralateral ear blocking did not convert CM directivity into a pressure response based on sound diffraction, as would be expected by eliminating the pressure gradient. No explanation can be given at present but perhaps the quality of the ear canal blocking may be an important factor in disrupting pressure gradients, since alternative sound paths may exist (Michelsen and Nocke 1974). Previous experiments on ear canal blocking in the barn owl have tested the effect on the accuracy of sound localization and changes in neuronal spatial receptive field properties but depend on stimulus frequency, goodness of fit and type of material (Knudsen and Konishi 1979, 1980). Further blocking experiments are needed to clearly demonstrate the possible effect of interaural sound transmission on ear directionality in the barn owl.

Auditory space and frequency

The role of frequency has not been recognized as an important factor for the mechanism of directional hearing in the barn owl (Knudsen and Konishi 1978b), although both the neural coding of auditory space and accurate sound localization depend on a restricted band of frequencies (Konishi 1973b; Knudsen et al. 1979; Knudsen and Konishi 1979). The present study shows that ear directionality depends intimately on the wavelength if, for example, movement of the CM axis is explained in terms of the maximum net pressure at the TM. This phenomenon would then involve the acoustical interference of sound waves originating from

the two input ports (ear canals), in contrast to the movement of the acoustic axis which is likely to depend on sound diffraction by the outer ear cavity. It is interesting to note that the region of frontal space mapped by the CM axis corresponds closely to the neural map in the auditory midbrain (Knudsen and Konishi 1978a, b), taking into consideration crossed pathways from the cochlea to the midbrain. The azimuthal limits of the best areas of space-mapped neurones range from 60° contralateral to 15° ipsilateral (Knudsen and Konishi 1978a, b) and a similar range is covered by the CM axis as frequency increases from 2–9 kHz. In both cases, there is binaural overlap of 15° about the midline, which is preserved at the forebrain level as well (Knudsen et al. 1977). If the suggestion of acoustic coupling between the eardrums is correct, then the interaural separation produces a CM axis for each ear which is very close to the midline and acoustic horizon, at the most accurately localized frequencies.

Acknowledgements. We thank N.H. Fletcher for helpful advice on the acoustical theory of ears, deriving horn equations and writing computer programs for the calculation of horn gain. Thanks are due to J.D. Pettigrew for assistance with the collection of owls.

References

- Autrum H (1942) Schallempfang bei Tier und Mensch. *Naturwissenschaften* 30:69–85
- Beranek LL (1954) *Acoustics*. McGraw-Hill, New York
- Chung S-H, Pettigrew A, Anson M (1978) Dynamics of the amphibian middle ear. *Nature* 272:142–147
- Coles RB, Guppy A (1986) Biophysical aspects of directional hearing in the Tammar wallaby (*Macropus eugenii*). *J Exp Biol* 121:371–394
- Coles RB, Lewis DB, Hill KG, Hutchings ME, Gower DM (1980) Directional hearing in the Japanese quail (*Coturnix coturnix japonica*). II. Cochlear physiology. *J Exp Biol* 86:153–170
- Fletcher NH, Thwaites S (1979) Physical models for the analysis of acoustical systems in biology. *Q Rev Biophys* 12:25–65
- Guppy A, Coles RB (1988) Acoustical and neural aspects of hearing in the Australian gleaning bats *Macroderma gigas* and *Nyctophilus gouldi*. *J Comp Physiol* 162:653–668
- Hill KG, Lewis DB, Hutchings ME, Coles RB (1980) Directional hearing in the Japanese quail (*Coturnix coturnix japonica*). I. Acoustic properties of the auditory system. *J Exp Biol* 86:135–151
- Knudsen EI (1980) Sound localization in birds. In: Popper AN, Fay RR (eds) *Comparative studies of hearing in vertebrates*. Springer, Berlin Heidelberg New York, pp 289–322
- Knudsen EI, Konishi M (1978a) A neural map of auditory space in the owl. *Science* 200:795–797
- Knudsen EI, Konishi M (1978b) Space and frequency are represented separately in auditory midbrain of the owl. *J Neurophysiol* 41:870–884
- Knudsen EI, Konishi M (1979) Mechanisms of sound localization in the barn owl (*Tyto alba*). *J Comp Physiol* 133:13–21

- Knudsen EI, Konishi M (1980) Monaural occlusion shifts receptive field locations of auditory midbrain units in the owl. *J Neurophysiol* 44:687–695
- Knudsen EI, Konishi M, Pettigrew JD (1977) Receptive fields of auditory neurons in the owl. *Science* 198:1278–1280
- Knudsen EI, Blasdel GG, Konishi M (1979) Sound localization by the barn owl (*Tyto alba*) measured with the search coil technique. *J Comp Physiol* 133:1–11
- Konishi M (1973a) How the owl tracks its prey. *Am Sci* 61:414–424
- Konishi M (1973b) Locatable and nonlocatable acoustic signals for barn owls. *Am Nat* 107:775–785
- Konishi M (1983) Neuroethology of acoustic prey localization in the barn owl. In: Huber F, Markl H (eds) *Neuroethology and behavioural physiology*. Springer, Berlin Heidelberg New York, pp 303–317
- Lewis DB, Coles RB (1980) Sound localization in birds. *Trends Neurosci* 3:102–105
- Michelsen A (1979) Insect ears as mechanical systems. *Am Sci* 67:696–706
- Michelsen A, Nocke H (1974) Biophysical aspects of sound communication in insects. *Adv Insect Physiol* 10:247–296
- Middlebrooks JC, Pettigrew JD (1981) Functional classes of neurons in the primary auditory cortex of the cat distinguished by sensitivity to sound location. *J Neurosci* 1:107–120
- Moiseff A, Konishi M (1981a) Neuronal and behavioural sensitivity to binaural time differences in the owl. *J Neurosci* 1:40–48
- Moiseff A, Konishi M (1981b) The owl's interaural pathway is not involved in sound localization. *J Comp Physiol* 144:299–304
- Norberg RA (1968) Physical factors in directional hearing in *Aegolius funereus* (Linné) (Strigiformes), with special reference to the significance of the asymmetry of the external ears. *Ark Zool* 20:181–204
- Norberg RA (1970) Hunting technique of Tengmalm's owl *Aegolius funereus*. *Ornis Scand* 1:51–64
- Norberg RA (1977) Occurrence and independent evolution of bilateral ear asymmetry in owls and implications on owl taxonomy. *Phil Trans R Soc Lond* 280:375–408
- Norberg RA (1978) Skull asymmetry, ear structure and function, and auditory localization in Tengmalm's owl, *Aegolius funereus* (Linné). *Phil Trans R Soc Lond* 282:325–410
- Olson HF (1947) *Acoustical engineering*. Van Nostrand, New York
- Payne RS (1971) Acoustic location of prey by barn owls (*Tyto alba*). *J Exp Biol* 54:535–573
- Pettigrew A, Chung SH, Anson M (1978) Neurophysiological basis of directional hearing in Amphibia. *Nature* 272:138–142
- Phillips DP, Calford MB, Pettigrew JD, Aitkin LM, Semple MN (1982) Directionality of sound pressure transformation at the cat's pinna. *Hearing Res* 8:13–28
- Rosowski JJ, Saunders JC (1980) Sound transmission through the avian interaural pathways. *J Comp Physiol* 136:183–190
- Schwartzkopf J (1962) Zur Frage des Richtungshörens von Eulen (Striges). *Z Vergl Physiol* 45:570–580
- Stellbogen E (1930) Über das äußere und mittlere Ohr des Waldkauzes (*Syrnium aluco* L.). *Z Morphol Ökol Tiere* 19:687–731
- Stresemann E (1934) *Handbuch der Zoologie*, vol 7, pt 2. Kükenthal W, Krumbach T (eds) De Gruyter, Leipzig pp 899
- Tiedemann F (1810) *Zoologie II, Anatomie und Naturgeschichte der Vögel*. Landshut
- Wada Y (1923) Beiträge zur vergleichenden Physiologie der Gehörorgane. *Pflügers Arch* 202:46–69